Urinary concentrating defect in mice with selective deletion of phloretin-sensitive urea transporters in the renal collecting duct

Robert A. Fenton*†, Chung-Lin Chou*, Gavin S. Stewart‡, Craig P. Smith‡§, and Mark A. Knepper*§

*Laboratory of Kidney and Electrolyte Metabolism, National Heart, Lung, and Blood Institute, National Institutes of Health, Bethesda, MD 20892; and ‡School of Biological Sciences, University of Manchester, Manchester M13 9PT, United Kingdom

Edited by Peter C. Agre, Johns Hopkins University School of Medicine, Baltimore, MD, and approved April 1, 2004 (received for review March 11, 2004)

To investigate the role of inner medullary collecting duct (IMCD) urea transporters in the renal concentrating mechanism, we deleted 3 kb of the UT-A urea transporter gene containing a single 140-bp exon (exon 10). Deletion of this segment selectively disrupted expression of the two known IMCD isoforms of UT-A, namely UT-A1 and UT-A3, producing *UT-A1/3*$^{-/-}$ mice. In isolated perfused IMCDs from *UT-A1/3*$^{-/-}$ mice, there was a complete absence of phloretin-sensitive or vasopressin-stimulated urea transport. On a normal protein intake (20% protein diet), *UT-A1/3*$^{-/-}$ mice had significantly greater fluid consumption and urine flow and a reduced maximal urinary osmolality relative to wild-type controls. These differences in urinary concentrating capacity were nearly eliminated when urea excretion was decreased by dietary protein restriction (4% by weight), consistent with the 1958 Berliner hypothesis stating that the chief role of IMCD urea transport in the concentrating mechanism is the prevention of urea-induced osmotic diuresis. Analysis of inner medullary tissue after water restriction revealed marked depletion of urea in *UT-A1/3*$^{-/-}$ mice, confirming the concept that phloretin-sensitive IMCD urea transporters play a central role in medullary urea accumulation. However, there were no significant differences in mean inner medullary Na^+ or Cl^- concentrations between *UT-A1/3*$^{-/-}$ mice and wild-type controls, indicating that the processes that concentrate NaCl were intact. Thus, these results do not corroborate the predictions of passive medullary concentrating models stating that NaCl accumulation in the inner medulla depends on rapid vasopressin-regulated urea transport across the IMCD epithelium.

UT-A | isolated perfused tubule | vasopressin | concentrating mechanism

For survival remote from water sources, terrestrial animals require effective water-conservation mechanisms. In birds and mammals, water conservation depends on specialized urinary concentrating mechanisms that reduce water excretion while maintaining solute excretion. This concentrating function is carried out in the renal medulla. In mammals, the medulla is divided into two regions, the outer medulla and the inner medulla (IM), both of which manifest increased tissue osmolality relative to the blood plasma (1). In these regions, high interstitial osmolality draws water from the renal collecting duct via aquaporin water channels, resulting in a concentrated final urine. In the outer medulla, the interstitial space is concentrated through the classic countercurrent multiplication mechanism (2) in which water and solute are separated by active NaCl transport from the water-impermeable thick ascending limb of Henle (3, 4). However, in the IM the ascending portion of Henle's loop is incapable of high rates of active transport (5, 6), implying that solute concentration in the IM occurs by a different, yet unknown mechanism.

One important feature of the IM that distinguishes it from the outer medulla is its ability to accumulate large amounts of urea. Berliner and coworkers (7, 8) originally proposed that urea accumulation in the IM occurs as a result of passive urea transport from the inner medullary collecting ducts (IMCDs). Further studies in isolated perfused IMCDs have established that the high urea permeability (P_{urea}) in the IMCD is due to the presence of phloretin-sensitive urea transporters in the IMCD cells (9–11).

In mammals, two urea transporter genes have been identified: UT-A (expressed in renal tubules and other epithelial tissues) and UT-B (expressed in erythrocytes and some endothelial cells). Several UT-A proteins are derived from the UT-A gene by the process of alternative splicing, including UT-A1 and UT-A3, expressed in the IMCD (12, 13), UT-A2, expressed in the thin descending limb of Henle (14), and UT-A5, expressed in testis (15). The UT-B gene encodes only a single protein, and recently UT-B-deficient mice, which manifest a defect in the urinary concentrating mechanism, have been generated (16).

Here we report the selective deletion of the collecting duct UT-A isoforms UT-A1 and UT-A3 (*UT-A1/3*$^{-/-}$ mice), resulting in the ablation of facilitated urea transport from the IMCD. After direct demonstration of the absence of phloretin-sensitive, vasopressin-regulated urea transport in isolated perfused IMCD segments, we have used the *UT-A1/3*$^{-/-}$ mice to address several longstanding questions regarding the physiology of the inner medullary concentrating mechanism: (*i*) Does urea accumulation in the IM depend on UT-A1 and UT-A3? (*ii*) Does water conservation depend on these urea transporters? (*iii*) Does the ability of the kidney to concentrate NaCl in the IM depend on rapid IMCD urea transport?

Methods

Construction of the Targeting Vector. By using the previously characterized structure of the mouse *UT-A* gene (17), a 12-kb targeting vector was constructed as illustrated in Fig. 1. Detailed information is included in *Supporting Text*, which is published as supporting information on the PNAS web site.

Generation of *UT-A1/3*$^{-/-}$ Mice. The targeting vector was linearized at a unique *Sal*I site and electroporated into CMT-1 embryonic stem (ES) cells; for selection, cells were grown in medium containing 200 μg/ml G418 and 2 μM gancyclovir. Correct targeting was identified by Southern analysis of genomic DNA using a probe flanking the 3′ end of the targeting vector and several restriction enzymes (Fig. 1). PCR analysis with primers situated both within the *pgk-neo* gene and outside the vector arms followed by sequencing confirmed correct targeting of the construct. Two positive ES cell clones were used to generate

This paper was submitted directly (Track II) to the PNAS office.

Abbreviations: IMCD, inner medullary collecting duct; P_{urea}, urea permeability; AVP, arginine vasopressin; IM, inner medulla; BW, body weight.

†To whom correspondence should be addressed at: National Institutes of Health, 10 Center Drive, Building 10, Room 6N260, Bethesda, MD 20892-1603. E-mail: fentonr@nhlbi.nih.gov.

§C.P.S. and M.A.K. contributed equally to this work.

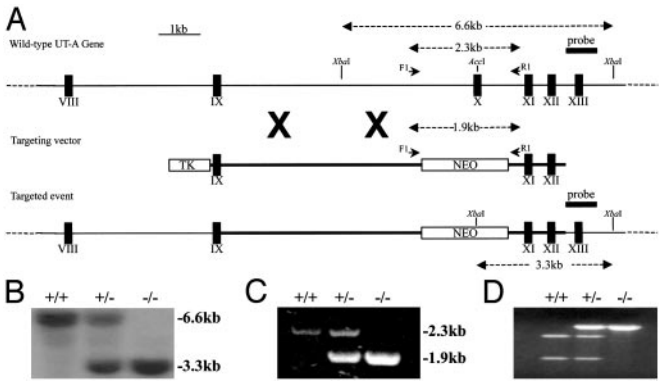

Fig. 1. Targeted disruption of the mouse *UT-A* gene. (*A*) Structure of the wild-type *UT-A* gene, the targeting vector, and the mutant allele. Exons are represented as filled boxes, and unique restriction enzyme sites are shown. The expression cassettes for the neomycin resistance gene (NEO) and thymidine kinase (TK) gene are shown as open boxes. Position of external probe and the length of restriction fragments and primers used for genotyping are denoted by arrows and arrowheads, respectively. (*B*) Representative Southern blot analysis of genomic DNA. *Xba*I-digested DNAs from wild-type, heterozygous, and *UT-A1/3*$^{-/-}$ mice were hybridized with probe as shown in *A*. Sizes (in kb) of bands are shown. (*C*) Representative results of PCR genotyping with primers (F1 and R1) as shown in *A*. Sizes (in kb) of bands are shown. (*D*) Restriction digestion of aforementioned PCR products with *Acc*I, unique to exon 10, results in the complete digestion of the wild-type PCR product, but not the knockout allele.

independent heterozygous founder animals by standard techniques; detailed information is included in *Supporting Text*. (All data presented are from one of these lines. Confirmatory studies done in the additional line were also consistent with the conclusions derived, although the demonstrated defect in water conservation was not as severe.) All animal procedures were approved by the National Heart, Lung, and Blood Institute Animal Care and Use Committee.

Isolated Perfused Tubule. P_{urea} was measured in terminal IMCD segments by using the isolated tubule perfusion technique (9). Detailed information is included in *Supporting Text*. In experiments requiring arginine vasopressin (AVP), the bath solution contained 5 nM AVP for 30 min before and during the measurements. Water-permeability measurements were performed as described previously (18). For all perfusion studies the investigator was blind to the genotype of the animal.

Immunoblotting. Protein preparation and immunoblotting were performed as previously described (19), by using affinity-purified, polyclonal antibodies targeted to different regions of UT-A proteins: mL446, raised to amino acids 57–75 of UT-A1; mQ2, raised to amino acids 444–461 of UT-A3; and L194, raised to amino acids 912–929 of UT-A1.

Immunocytochemistry. The technique for fixation, sectioning, and immunoperoxidase staining of the kidney has been described in detail elsewhere (20). Light microscopy was performed with a Nikon Eclipse E800 upright microscope, and exposure settings were identical among the groups.

Northern Blot Analysis. Kidney IM and testis were dissected from wild-type, heterozygous, and *UT-A1/3*$^{-/-}$ mice, and RNA was extracted by using the RiboPure kit (Ambion, Austin, TX). Blotting and hybridization were performed as described previously (21) with a full-length UT-A1 cDNA probe (GenBank accession no. AF366052).

RT-PCR, cDNA Cloning, and Oocyte Expression. Total RNA from kidney IM was reverse transcribed, and PCR was performed as described previously (22). For PCR, the forward gene specific primer was situated in exon 8 of the UT-A gene, and the reverse primer was situated in exon 13. Mutant PCR fragments were subcloned into full-length UT-A1 or UT-A3 cDNAs, replacing the corresponding region, and sequenced. Expression of the mutant clones, termed UT-A1$^{(10-)}$ and UT-A3$^{(10-)}$, in *Xenopus* oocytes was performed as described (21).

Metabolic Cage Studies. Five wild-type and *UT-A1/3*$^{-/-}$ mice were maintained in mouse metabolic cages (Hatteras Instruments, Cary, NC) for the duration of the study, under controlled temperature and light conditions (12-h light and dark cycles), and two experimental manipulations were performed.

Twenty-Percent Protein Diet. Initially, all mice received a fixed daily ration of 5 g of gelled diet per 20 g of body weight (BW) per day containing 20% protein by weight (as casein). The gelled diet (per 5 g total) was made up of 1 ml of deionized water, 4 g of special low-salt (NaCl) synthetic food [0.001% Na (wt/wt); Research Diets (New Brunswick, NJ)], 0.2 mmol NaCl, and 25 mg of agar. Preweighed drinking water was provided ad libitum during the initial period of the study. After 3 days of adaptation to the cages and diet, urine was collected under mineral oil in preweighed collection vials for five successive 24-h periods. Urine volume was measured gravimetrically, by assuming a density of one. After the initial collection period, each mouse received a fixed daily ration of 5.7 g of gelled diet per 20 g of BW per day for 24 h, containing 1.7 ml of deionized water. Mice did not have access to supplemental drinking water during this period. Urine was collected under mineral oil in preweighed collection vials for a 24-h period.

Four-Percent Protein Diet. The study was performed exactly as detailed above, except that mice were given a diet containing only 4% protein by weight (as casein) with no other source of protein. The starch and sucrose content of the diet was altered in inverse proportion to casein to ensure an equivalent calorie intake.

Solute Content of IM. Five wild-type and *UT-A1/3*$^{-/-}$ mice were maintained in mouse metabolic cages on a 20% protein diet for 5 days, before water restriction to 1.7 ml per 20 g of BW per day as detailed above. Tissue was processed by using a modified method based on the work of Schmidt-Nielsen *et al.* (23); detailed information is included in *Supporting Text*. Sodium and potassium concentrations were determined by using a flame spectrophotometer (Instrumentation Laboratory, Lexington, MA), chloride concentration was determined by using a chloridometer, and a commercially available assay was used to determine urea concentration (Biotron Diagnostics, Hemet, CA).

Results

To selectively disrupt the collecting duct urea transporters UT-A1 and UT-A3, a targeting vector in which exon 10 was replaced by a neomycin expression cassette was constructed and used for gene targeting (Fig. 1*A*). Exon 10 codes for amino acids 291–339 of UT-A1 and is situated in a large hydrophobic region, thought to be membrane-spanning (24). Deletion of this exon and splicing from exons 9 to 11 is predicted to result in a frameshift. Southern blot analysis of mouse genomic DNA demonstrated a 6.6-kb fragment in wild-type mice, 6.6- and 3.3-kb fragments in heterozygous mice, and a 3.3-kb fragment in *UT-A1/3*$^{-/-}$ mice (Fig. 1*B*). Correct targeting of the construct was confirmed by PCR, restriction digestion, and sequencing (Fig. 1 *C* and *D*).

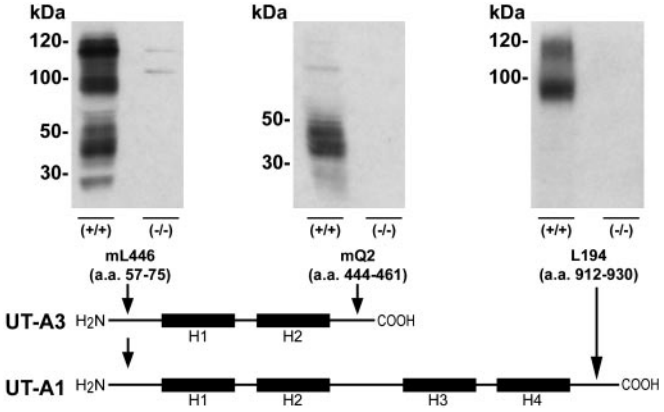

Fig. 2. Representative immunoblots of whole IM homogenates probed with several isoform-selective polyclonal antibodies. The schematic diagram shows the antibodies used and the protein isoforms they detected. H1–H4 shows putative membrane-spanning regions. When using antibody mL446, strong protein bands of ≈100 and 120 kDa (glycosylated forms of UT-A1) and a protein ''smear'' between 40 and 56 kDa (glycosylated UT-A3) are absent from *UT-A1/3*$^{-/-}$ mice. When using antibody mQ2, which selectively recognizes UT-A3, a protein smear between 40 and 56 kDa is absent in *UT-A1/3*$^{-/-}$ mice. When using antibody L194, strong protein bands of ≈100 and 120 kDa (UT-A1) are absent in *UT-A1/3*$^{-/-}$ mice.

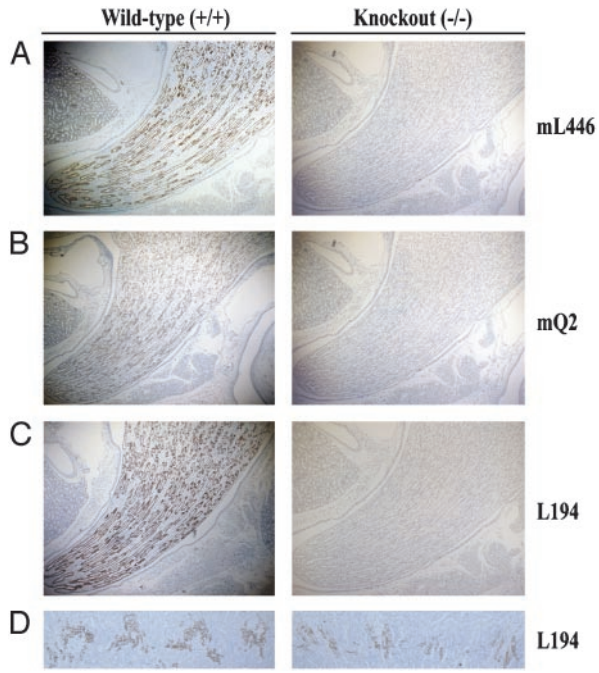

Fig. 3. Immunocytochemistry using polyclonal antibodies as depicted in Fig. 2. No labeling of the *UT-A1/3*$^{-/-}$ IM is seen with mL446 (*A*), mQ2 (*B*), or L194 (*C*). (*D*) No reduction in the intensity of UT-A2 labeling in the thin descending limbs of Henle's loop is observed.

From the initial heterozygote crosses, 69 wild-type mice, 129 heterozygote offspring, and 61 *UT-A1/3*$^{-/-}$ mice were observed (132 males and 127 females), consistent with a 1:2:1 Mendelian pattern. No differences in physical appearance, BW, or behavior were detectable between the *UT-A1/3*$^{-/-}$ mice and littermate controls. Despite the deletion of UT-A5 (*vide infra*), a testis-specific isoform that contains exon 10, all *UT-A1/3*$^{-/-}$ mice bred normally, with no evidence of impaired fertility.

Immunoblots of whole IM with antibodies targeted to the NH_2 terminus of UT-A1 (antibody mL446), the COOH terminus of UT-A3 (antibody mQ2), or the COOH terminus of UT-A1 (antiserum L194) revealed no evidence of UT-A1 or UT-A3 protein in *UT-A1/3*$^{-/-}$ knockout animals (representative blots are shown in Fig. 2). Immunocytochemistry with the same antibodies revealed no staining of the IMCD in *UT-A1/3*$^{-/-}$ mice (Fig. 3 *A–C*). Antiserum L194 also recognizes UT-A2, which is expressed chiefly in outer medullary thin descending limbs (14). As shown in Fig. 3*D*, there was no obvious difference in intensity of outer medullary UT-A2 labeling between wild-type and *UT-A1/3*$^{-/-}$ mice.

P_{urea} values measured in isolated perfused terminal IMCDs from *UT-A1/3*$^{-/-}$ mice were substantially lower than in IMCDs from wild-type mice (Fig. 4*A*) and were equivalent to values expected because of the simple lipid-phase diffusion of urea (10). Furthermore, AVP significantly increased P_{urea} in terminal IMCDs from wild-type mice (37 ± 7.8 versus $92 \pm 6.6 \times 10^{-5}$ cm/s, respectively; $P < 0.001$), whereas in *UT-A1/3*$^{-/-}$ mice no response to vasopressin was observed (Fig. 4*A*). Further perfusion experiments were performed to determine the effects of phloretin, an inhibitor of facilitative urea transport (9), on the P_{urea} in *UT-A1/3*$^{-/-}$ and wild-type mice. In wild-type mice, 0.1 nM AVP caused a significant increase in P_{urea} (27 ± 5.2 versus $98 \pm 8 \times 10^{-5}$ cm/s, respectively; $P < 0.001$), and addition of 0.25 mM phloretin, still in the presence of AVP, to both the apical and basolateral side of the tubules resulted in a significant decrease in P_{urea} (Fig. 4*B*). In littermate *UT-A1/3*$^{-/-}$ mice, AVP had no significant effect on the P_{urea}, and the low permeability observed was not inhibited by phloretin, suggesting that it was not due to a known facilitative urea transporter. In contrast, AVP (0.1 nM) markedly increased the osmotic water permeability in isolated perfused IMCDs from *UT-A1/3*$^{-/-}$ mice from 113 ± 35 to $372 \pm 75 \times 10^{-4}$ cm/s ($P < 0.05$), indicating that the vasopressin signaling cascade was intact (Fig. 4*C*).

Northern blot analysis of kidney inner medullary RNA with a full-length UT-A1 cDNA probe revealed nearly the same size mRNA transcripts in wild-type and *UT-A1/3*$^{-/-}$ mice (Fig. 5*A*), compatible with the small size (148 bp) of the deleted exon. The approximate sizes of the transcripts observed, 4.0, 3.0, and 2.1 kb, are consistent with those reported for full-length UT-A1, UT-A2, and UT-A3, respectively (21). When an equivalent probe was hybridized to testis RNA, a strong signal representing UT-A5 was observed at 1.4 kb in wild-type mice, but signals centered at 0.6 kb, representing truncated mRNA transcripts, were observed for *UT-A1/3*$^{-/-}$ mice (Fig. 5*B*). RT-PCR and sequencing revealed that in the kidney IM of *UT-A1/3*$^{-/-}$ mice, exon 9 of the UT-A gene was directly spliced to exon 11. These "exon 10-deleted" cDNAs [termed UT-A1$^{(10-)}$ and UT-A3$^{(10-)}$] were cloned and expressed in *Xenopus* oocytes ($n = 10$ for each group), confirming that the deletion of exon 10 resulted in the loss of phloretin-sensitive urea transport (see Fig. 8, which is published as supporting information on the PNAS web site, and *Supporting Text*).

Berliner *et al*. (8) proposed a hypothesis that assigns a role for a specific IMCD urea transport pathway in the urinary concentrating mechanism. They suggested that the large amount of urea normally excreted by the mammalian kidney would require large amounts of water for its removal unless urea's osmotic effect in the lumen were somehow negated. They further proposed that urea in the lumen of the IMCD would have no osmotic effect if urea accumulates to the same concentration in the inner medullary interstitium. They emphasized that this condition could be created if the IMCD were to possess an extremely high permeability to urea, allowing rapid equilibration of urea concentration across the IMCD. The Berliner hypothesis predicts that deletion of specialized urea transporters from the IMCD would result in an impaired capacity to conserve water, owing to the osmotic effect of urea in the lumen. To test this hypothesis, the

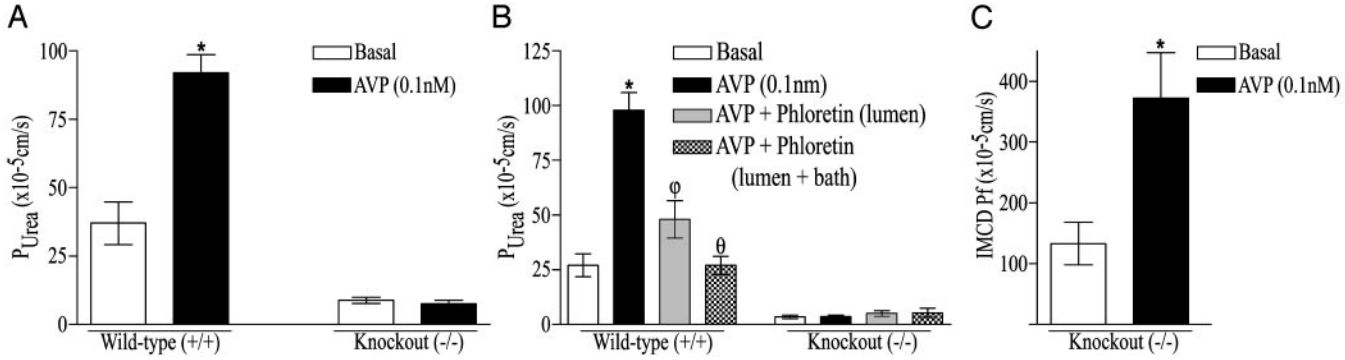

Fig. 4. P_{urea} in the IMCD of *UT-A1/3*$^{-/-}$ mice. (*A*) Effect of 0.1 nM AVP on P_{urea}. Five tubules from age-matched wild-type and *UT-A1/3*$^{-/-}$ littermates were perfused for each group. *, Significant change between groups. (*B*) Effect of 0.25 mM phloretin on P_{urea} in the presence of AVP. Symbols represent a significant change in P_{urea} from the preceding perfusion group. Tubules from five age-matched wild-type and *UT-A1/3*$^{-/-}$ littermates were perfused for each group. (*C*) The effect of 0.1 nM AVP on transepithelial, osmotic water permeability (Pf) in isolated perfused IMCD segments of *UT-A1/3*$^{-/-}$ mice. Six tubules were perfused for each group. *, Significant change between groups.

urinary concentrating function of *UT-A1/3*$^{-/-}$ mice on a 20% protein diet was measured. Under basal conditions, with free access to drinking water, *UT-A1/3*$^{-/-}$ mice exhibited significantly greater fluid consumption (6.3 ± 0.34 versus 2.7 ± 0.23 ml/day) and urine flow (4.4 ± 0.20 ml/day versus 1.5 ± 0.12 ml/day) (Fig. 6*A*). Urine osmolality [861 ± 22 milliosmol (mosmol)/kg H_2O] in *UT-A1/3*$^{-/-}$ mice was also significantly lower than in wild-type mice (2,317 ± 80 mosmol/kg H_2O) (Fig. 6*A*). Furthermore, after a 24-h water restriction (1.7 ml of water per day per 20 g of BW), *UT-A1/3*$^{-/-}$ mice exhibited no ability to decrease urine flow and could not significantly raise their maximal urinary osmolality above that observed under basal conditions (Fig. 6*A*). During this 24-h water restriction, BW decreased by 21 ± 0.3% in *UT-A1/3*$^{-/-}$ mice ($n = 5$) compared with 4.3 ± 1.2% in wild-type mice.

The Berliner hypothesis predicts that this defect in water conservation should be ameliorated when urea excretion is decreased as a result of dietary protein restriction. Indeed, on a low-protein diet (4% by weight) after a 24-h water restriction, although *UT-A1/3*$^{-/-}$ mice still had a somewhat greater urine flow and lower maximal urine osmolality, the urinary concentrating defect observed compared with that in wild-type mice was nearly eliminated (Fig. 6*B*).

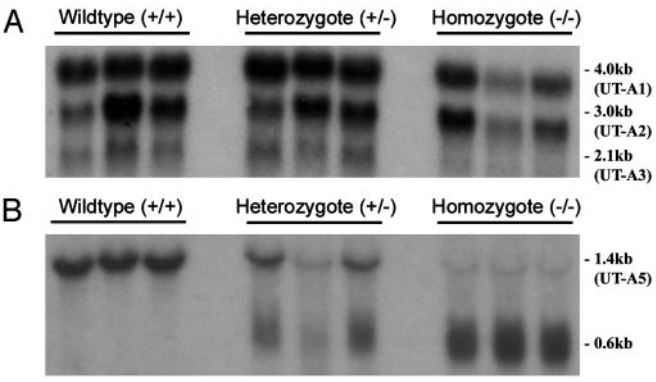

Fig. 5. Comparison of UT-A transcripts in wild-type and *UT-A1/3*$^{-/-}$ mice. Each lane represents a sample from a different mouse. (*A*) Northern blot of kidney IM total RNA (3 μg per lane) probed with a full-length UT-A1 cDNA probe at high stringency. Strong hybridization to mRNA species is evident at ≈4.0 and 2.1 kb in both wild-type and *UT-A1/3*$^{-/-}$ mice. (*B*) Northern blot of testis total RNA (15 μg per lane) probed with a full-length UT-A1 cDNA probe at high stringency. In wild-type mice, strong signals representing UT-A5 are evident at 1.5 kb. In contrast, *UT-A1/3*$^{-/-}$ mice only express truncated transcripts.

Because the ascending limb of the loop of Henle seems incapable of rapid NaCl transport in the IM, the classical countercurrent multiplier model of Kuhn and Ramel (2), which concentrates NaCl in the outer medulla, apparently does not play a role in the accumulation of NaCl in the IM. Various hypotheses have been offered to explain NaCl accumulation in the IM, including a proposal that the accumulation of NaCl relies on a series of passive transport processes critically dependent on rapid, passive transport of urea across the IMCD epithelium (25, 26). These hypotheses predict that deletion of specific urea transporters from the IMCD should impair the concentration of NaCl in the IM. To test this prediction we measured the mean urea, Na^+, Cl^-, and K^+ concentrations in IM of *UT-A1/3*$^{-/-}$ mice and wild-type littermates (Fig. 7). These measurements were made in water-restricted mice on a 20% protein intake, a condition that virtually maximizes urinary concentrating ability. In *UT-A1/3*$^{-/-}$ mice there was a significantly lower inner medullary urea concentration (Fig. 7), confirming the view that urea accumulation in the IM depends on urea transporters in the IMCD. However, there was no reduction in the mean Na^+ concentration in inner medullary tissue. Therefore, these observations fail to corroborate the view that inner medullary Na^+ accumulation depends on facilitated urea transport in the IMCD. Furthermore, Cl^- and K^+ concentrations were unchanged in the IM of *UT-A1/3*$^{-/-}$ mice compared with wild-type animals.

Discussion

To clarify the role of UT-A urea transporters in the renal concentrating mechanism, we deleted 3 kb of the UT-A gene containing a single 148-bp exon (exon 10). Deletion of this segment selectively disrupted a region encoding segments of two IMCD isoforms of UT-A, namely UT-A1 and UT-A3 (17). Successful deletion of these transporters was confirmed by immunoblotting and immunocytochemistry, demonstrating that UT-A1 and UT-A3 proteins were absent from the IM of *UT-A1/3*$^{-/-}$ mice, and by isolated perfused tubule studies showing an absence of phloretin-sensitive and vasopressin-regulated urea transport in IMCD segments. Thus, we conclude that UT-A1 and UT-A3 mediate phloretin-sensitive, vasopressin-regulated urea transport in the IMCD.

The selective deletion of IMCD urea transport mechanisms provided an ideal mouse model to address the role of inner medullary urea transporters in the urinary concentrating process. Contemporary thinking on the contribution of urea trans-

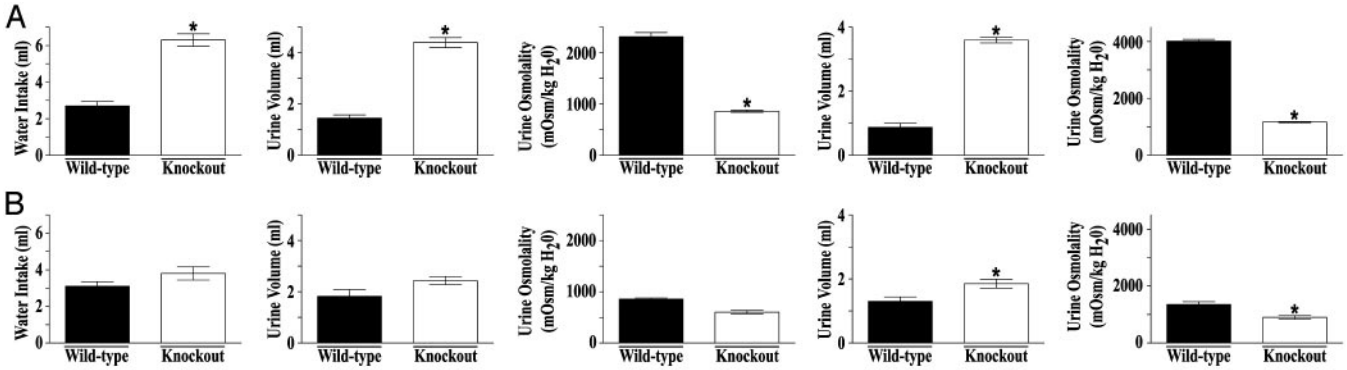

Fig. 6. Water conservation and urinary concentrating ability of *UT-A1/3*$^{-/-}$ mice. For all graphs, values are mean ± SE. *, Significant difference between wild-type (filled bars) and *UT-A1/3*$^{-/-}$ (open bars) mice. (*A*) Values obtained when mice received a 20% protein diet. (*B*) Identical studies performed on a 4% protein diet. Graphs show 24-h water consumption, urine output under basal conditions (free access to drinking water), urine osmolality under basal conditions, urine output after a 24-h water restriction, and maximal urinary osmolality after a 24-h water restriction.

porters to the urinary concentrating mechanism is based largely on a fundamental model of urea handling proposed >45 years ago by Berliner *et al*. (8). Recognizing that large amounts of urea are formed in the mammalian liver and that this urea constitutes a large osmotic load that must be excreted by the kidneys, their studies addressed the question of why the excretion of so much urea did not obligate large amounts of water excretion, as equivalent osmotic loads of almost any other solute would. Their model proposed that luminal urea in the IMCD is osmotically ineffective because of a high IMCD P_{urea} that, abetted by countercurrent exchange processes, allows urea to accumulate to high concentrations in the inner medullary interstitium. In studies conducted in isolated rat renal IM, Berliner and coworkers (7) demonstrated that the IMCD has this requisite high P_{urea}. Subsequently, our laboratory demonstrated that specialized phloretin-sensitive urea transporters mediate this rapid urea transport in the IMCD (9, 10); these studies led to the cloning of urea transporter cDNAs (27–29). The results of the present study corroborated the major features of the Berliner model. On a "normal" level of protein intake (20% protein), renal water conservation was markedly impaired in *UT-A1/3*$^{-/-}$ compared with wild-type control mice. However, when the protein intake was decreased to 4% of the total dietary mass, markedly reducing the urea load to the kidneys, the apparent difference in water conservation between *UT-A1/3*$^{-/-}$ and wild-type control mice was virtually abolished (Fig. 6). Therefore, we conclude that the concentrating defect seen in *UT-A1/3*$^{-/-}$ mice depends on the excretion of a large amount of urea. An additional observation of the present study is that urea accumulation in the IM was significantly impaired in *UT-A1/3*$^{-/-}$ mice (Fig. 7), which is also consistent with the proposal by Berliner *et al.* (8) that urea accumulation in the inner medullary interstitium depends on rapid transport of urea from the IMCD lumen.

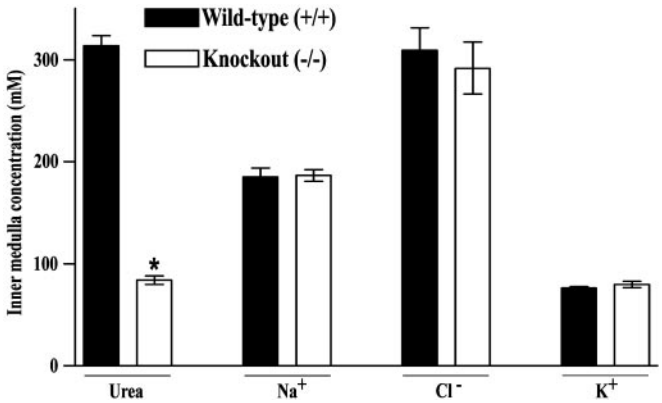

Fig. 7. Comparison of inner medullary solute composition of wild-type and *UT-A1/3*$^{-/-}$ mice. For each group, 10 kidney IM were used to determine the urea, sodium, chloride, and potassium concentrations. Values are mean ± SE. *, Significant difference between the groups.

It has long been recognized that urea and NaCl comprise most of the osmoles that accumulate in the inner medullary interstitium (1). Elucidating the mechanisms by which NaCl accumulates has been a subject of considerable controversy. One influential idea on this question, offered in 1972 by Stephenson (25) and by Kokko and Rector (26), was that the energy required for NaCl accumulation in the IM is derived indirectly from rapid urea transport from the IMCD. Our present findings do not corroborate this view. When mice were maintained on a 20% protein diet and water-restricted, we observed no significant difference in the mean concentrations of Na^+ or Cl^- in inner medullas from *UT-A1/3*$^{-/-}$ versus wild-type control mice, despite a substantial impairment of inner medullary urea accumulation.

Due to the complex nature of alternative splicing mechanisms within the UT-A gene, deletion of exon 10 also resulted in the loss of a testis-specific isoform, UT-A5. An important conclusion of the present study is that male fertility does not depend on UT-A5 expression in testis. In testis RNA, only mRNA species corresponding to truncated UT-A5 transcripts were detected, indicating a lack of exon 9–11 splicing in this tissue. Several testis-specific alternative splicing mechanisms that result in regulation of gene expression have previously been uncovered (30). Our results are consistent with the view that, for the UT-A gene, alternative splicing mechanisms are regulated in a tissue-specific manner.

In conclusion, we have generated UT-A urea transporter knockout mice, providing a mouse model to examine the role of urea transporters in both renal and extrarenal tissues. *UT-A1/3*$^{-/-}$ mice exhibit a severe defect in their capacity for renal water conservation, which is ameliorated by a low-protein diet. Furthermore, we have determined that a passive inner medullary concentrating system that relies on urea accumulation in the IMCD, originally proposed by Stephenson (25) and Kokko and Rector (26), appears unlikely to be the mechanism by which NaCl accumulates in the inner medullary interstitium.

We thank Chengyu Liu (National Heart, Lung, and Blood Institute Transgenic Core Facility at the National Institutes of Health) for expert assistance; Christian Combs (National Heart, Lung, and Blood Institute

Light Microscopy Core Facility); Christopher Cottingham; and William Brandt and Anneliese Flynn for technical assistance. This work was supported by the National Institutes of Health, Intramural Budget of the National Heart, Lung, and Blood Institute, Project Z01-HL-01282-KE (to M.A.K.) and by Royal Society and Biotechnology and Biological Sciences Research Council Grant 34/D10935 (to C.P.S.).

1. Ullrich, K. J. & Jarausch, K. H. (1957) *Pflügers Arch.* **262,** S537–S550.
2. Kuhn, W. & Ramel, A. (1959) *Helv. Chim. Acta* **42,** 628–660.
3. Rocha, A. S. & Kokko, J. P. (1973) *J. Clin. Invest.* **52,** 612–624.
4. Burg, M. B. & Green, N. (1973) *Am. J. Physiol.* **224,** 659–668.
5. Imai, M. & Kokko, J. P. (1974) *J. Clin. Invest.* **53,** 393–402.
6. Marsh, D. J. & Azen, S. P. (1975) *Am. J. Physiol.* **228,** 71–79.
7. Morgan, T., Sakai, F. & Berliner, R. W. (1968) *Am. J. Physiol* **214,** 574–581.
8. Berliner, R. W., Levinsky, N. G., Davidson, D. G. & Eden, M. (1958) *Am. J. Med.* **24,** 730–744.
9. Chou, C. L. & Knepper, M. A. (1989) *Am. J. Physiol.* **257,** F359–F365.
10. Sands, J. M., Nonoguchi, H. & Knepper, M. A. (1987) *Am. J. Physiol.* **253,** F823–F832.
11. Sands, J. M. & Knepper, M. A. (1987) *J. Clin. Invest.* **79,** 138–147.
12. Terris, J. M., Knepper, M. A. & Wade, J. B. (2001) *Am. J. Physiol. Renal. Physiol.* **280,** F325–F332.
13. Nielsen, S., Terris, J., Smith, C. P., Hediger, M. A., Ecelbarger, C. A. & Knepper, M. A. (1996) *Proc. Natl. Acad. Sci. USA* **93,** 5495–5500.
14. Wade, J. B., Lee, A. J., Liu, J., Ecelbarger, C. A., Mitchell, C., Bradford, A. D., Terris, J., Kim, G. H. & Knepper, M. A. (2000) *Am. J. Physiol. Renal. Physiol.* **278,** F52–F62.
15. Fenton, R. A., Howorth, A., Cooper, G. J., Meccariello, R., Morris, I. D. & Smith, C. P. (2000) *Am. J. Physiol.* **279,** C1425–C1431.
16. Yang, B., Bankir, L., Gillespie, A., Epstein, C. J. & Verkman, A. S. (2002) *J. Biol. Chem.* **277,** 10633–10637.
17. Fenton, R. A., Cottingham, C. A., Stewart, G. S., Howorth, A., Hewitt, J. A. & Smith, C. P. (2002) *Am. J. Physiol. Renal. Physiol.* **282,** F630–F638.
18. Chou, C. L., Ma, T., Yang, B., Knepper, M. A. & Verkman, A. S. (1998) *Am. J. Physiol.* **274,** C549–C554.
19. Terris, J., Ecelbarger, C. A., Nielsen, S. & Knepper, M. A. (1996) *Am. J. Physiol.* **271,** F414–F422.
20. Fenton, R. A., Chou, C. L., Ageloff, S., Brandt, W., Stokes, J. B. & Knepper, M. A. (2003) *Am. J. Physiol. Renal. Physiol.* **285,** F143–F151.
21. Fenton, R. A., Stewart, G. S., Carpenter, B., Howorth, A., Potter, E. A., Cooper, G. J. & Smith, C. P. (2002) *Am. J. Physiol. Renal. Physiol.* **283,** F817–F825.
22. Fenton, R. A., Cooper, G. J., Morris, I. D. & Smith, C. P. (2002) *Am. J. Physiol.* **282,** C1492–C1501.
23. Schmidt-Nielsen, B., Graves, B. & Roth, J. (1983) *Am. J. Physiol.* **244,** F472–F482.
24. Sands, J. M. (2003) *Annu. Rev. Physiol.* **65,** 543–566.
25. Stephenson, J. L. (1972) *Kidney Int.* **2,** 85–94.
26. Kokko, J. P. & Rector, F. C. (1972) *Kidney Int.* **2,** 214–223.
27. Smith, C. P., Lee, W. S., Martial, S., Knepper, M. A., You, G., Sands, J. M. & Hediger, M. A. (1995) *J. Clin. Invest.* **96,** 1556–1563.
28. You, G., Smith, C. P., Kanai, Y., Lee, W. S., Stelzner, M. & Hediger, M. A. (1993) *Nature* **365,** 844–847.
29. Karakashian, A., Timmer, R. T., Klein, J. D., Gunn, R. B., Sands, J. M. & Bagnasco, S. M. (1999) *J. Am. Soc. Nephrol.* **10,** 230–237.
30. Venables, J. P. (2002) *Curr. Opin. Genet. Dev.* **12,** 615–619.